ELSEVIER

Colloids and Surfaces
A: Physicochemical and Engineering Aspects 187–188 (2001) 523–529

COLLOIDS AND SURFACES A

www.elsevier.nl/locate/colsurfa

Freezing behavior in porous glasses and MCM-41

Malgorzata Sliwinska-Bartkowiak [a,*], Grazyna Dudziak [a], Roman Gras [a], Roman Sikorski [a], Ravi Radhakrishnan [b], Keith E. Gubbins [b,1]

[a] *Instytut Fizyki, Uniwersytet im Adama Mickiewicza, Umultowska 85, 61-61 4 Poznan, Poland*
[b] *North Carolina State University, 113 Riddick Labs, Raleigh, NC 27695, USA*

Abstract

We report experimental measurements of the melting and freezing behavior of fluids in nano-porous media. The experimental studies are for nitrobenzene in the silica based pores of controlled pore glass (CPG), Vycor and MCM-41. Dielectric relaxation spectroscopy was used to determine melting points and the orientational relaxation times of the nitrobenzene molecules in the bulk and the confined phase. It was found that the confined fluid freezes into a single crystalline structure for average pore diameters greater than 20 σ, where σ is the diameter of the fluid molecule. For average pore sizes between 20 and 15 σ, part of the confined fluid freezes into a frustrated crystal structure with the rest forming an amorphous region. For pore sizes smaller than 15 σ, even the partial crystallization did not occur.

Keywords: Freezing behavior; Porous glasses; MCM-41

1. Introduction

There have been numerous experimental studies on freezing of simple fluids in silica based pores [1]. Experiments on freezing that have used porous silica glass as the confinement medium have always resulted in a decrease in the freezing temperature, T_f, as compared to the bulk. In view of this large body of experimental evidence for a decrease in the freezing temperature due to confinement, it is tempting to assume that a decrease always occurs. However, in a subsequent molecular simulation study of freezing of simple fluids in slit pores, Miyahara and Gubbins [2] showed that T_f was strongly affected by the strength of the attractive forces between the fluid molecules and the pore walls. For repulsive or weakly attractive potentials, T_f decreased. For strongly attracting walls such as carbons, an *increase* in T_f was observed. Moreover, the increase in T_f was predicted to be larger for slit than cylindrical pores [3]. Recently, Radhakrishnan et. al. [4] computed the global freezing diagram for a Lennard–Jones fluid, and showed the dependence of the freezing temperature on the relative strengths of the fluid–wall to the fluid–fluid strengths. The authors also verified some of the predictions by conducting experimental studies on CCl_4 and nitrobenzene

* Corresponding author.
E-mail addresses: msb@main.amu.edu.pl (M. Sliwinska-Bartkowiak), keg@ncsu.edu (K.E. Gubbins).
[1] Tel.: +1-919-5132262.

0927-7757/01/$ - see front matter
PII: S0927-7757(01)00637-9

freezing in porous silica and activated carbon fibers (ACF).

In this paper, we study the freezing behavior and structure of the confined fluid phases in cylindrical (MCM-41) and networked porous systems (CPG and Vycor), using dielectric relaxation spectroscopy. The objective is to compare and contrast the freezing behavior of confined fluids in slit-shaped pores and cylindrical pores.

2. Experimental methods

The nitrobenzene samples were reagent grade chemicals, and were distilled twice at reduced pressure prior to use in the experiment. Nitrobenzene was further dried over Al_2O_3, centrifuged, and stored in the absence of light to avoid contamination by photochemical reactions. The conductivities of the purified nitrobenzene samples were found to be less than 10^{-10} ohm^{-1} m^{-1}. The porous silica samples used were the commercially available controlled pore glass (CPG) from CPG, with a pore size distribution of about 5% around the mean pore diameter [5]. Different CPG samples having average pore diameters ranging from 50 to 7.5 nm were used. We also studied confinement effects in Vycor glass from Corning, having a mean pore size of 4.5 nm [6], and a silica-based MCM-41 material with mean pore diameter of 2.8 nm. The pore samples were kept under vacuum prior to and during the introduction of the fluid. The MCM-41 samples were synthesized at A. Mickiewicz University, and were characterized using x-ray diffraction and nitrogen adsorption measurements [7]. The characterization results for MCM-41 showed that these crystalline materials consisted of uniform pores in a hexagonal arrangement with a narrow pore size distribution (dispersion less than 5%) [7]. The average pore sizes for the controlled pore glass and Vycor samples were inferred from mercury intrusion porosimetry, while that for the MCM-41 samples were inferred from nitrogen adsorption measurements [5–7].

2.1. Dielectric relaxation spectroscopy (DS)

The complex dielectric permittivity $\kappa^* = \kappa_r - i\kappa_i$, is measured as a function of temperature and frequency [8]. For an isolated dipole rotating under an oscillating electric field in a viscous medium, the Debye dispersion relation is derived using classical mechanics:

$$\kappa^* = \kappa_{\infty,r} + \frac{\kappa_{s,r} - \kappa_{\infty,r}}{1 + i\omega\tau} \quad (1)$$

Here ω is the frequency of the applied potential and τ is the orientational (rotational) relaxation time of a dipolar molecule. The subscript s refers to static permittivity (low frequency limit, when the dipoles have sufficient time to be in phase with the applied field). The subscript ∞ refers to the optical permittivity (high frequency limit) and is a measure of the induced component of the permittivity. Further details of the experimental methods are described elsewhere [8,9]. The dielectric relaxation time was calculated by fitting the dispersion spectrum of the complex permittivity near resonance to the Debye model of orientational relaxation.

3. Results

3.1. Dielectric relaxation

The capacitance C and tangent loss tan (δ) were measured as a function of frequency and temperature for bulk nitrobenzene and for nitrobenzene adsorbed in CPG, Vycor and MCM-41 materials of different pore sizes, ranging from 50 to 2.4 nm, from which the dielectric constant $\kappa_r(T, \omega)$ and the loss factor $\kappa_i(T, \omega)$ were calculated [8]. The dielectric constant is a natural choice of order parameter to study freezing of dipolar liquids, because of the large change in the orientational polarizability between the liquid and solid phases. The melting point can be taken to be the temperature at which there is a large increase in the permittivity, as the solid phase is heated. The spectrum of the complex permittivity (κ_r, κ_i vs. ω) is fit to the dispersion relation (Eq. (1)), to determine the dielectric relaxation time τ. The frequency range in this study (100 Hz–10 MHz) is expected to encompass the resonant frequencies corresponding to the dielectric relaxation in the solid phases and glass-like phases. According to equation Eq. (1), the κ_r function

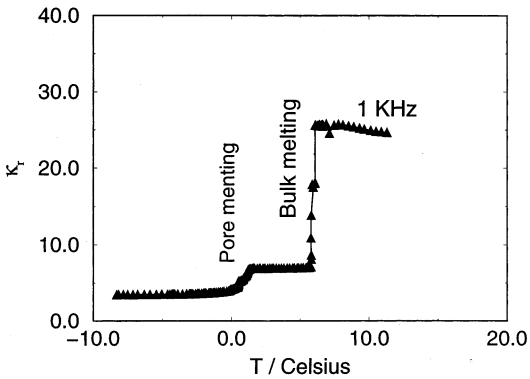

Fig. 1. The behavior of κ_r vs. T for bulk nitrobenzene. The sharp increase at 5.6°C corresponds to bulk melting.

shows a point of inflection and the κ'' function goes through a maximum at the resonant frequency. Therefore, from a spectrum plot of κ_r, κ_i vs. $\log_{10}(\omega)$, the relaxation time can be calculated as the reciprocal of the frequency corresponding to a saddle point of the κ_r function or a maximum of the κ_i function.

For nitrobenzene confined in CPG, the sample is introduced between the capacitor plates as a suspension of nitrobenzene filled CPG particles in pure nitrobenzene. Therefore, the capacitance measurement yields an effective relative permittivity of the suspension of CPG in pure nitrobenzene. For a CPG sample with average pore diameter of 25 nm, κ_r experiences two sudden changes (Fig. 1). The sharp increase at 2°C is attributed to melting in the pores, while that at 5.6°C corresponds to the bulk melting. The frequency spectrum at a particular temperature is used to obtain the orientational relaxation times in the different phases of the system as described before.

3.2. Maxwell–Wagner effect

The behavior of the relaxation times as a function of temperature for nitrobenzene in CPG of 25 nm pore size are depicted in Fig. 2. For temperatures greater than 2°C (melting point inside the pores), there are two different relaxations; they manifest themselves as a double inflection

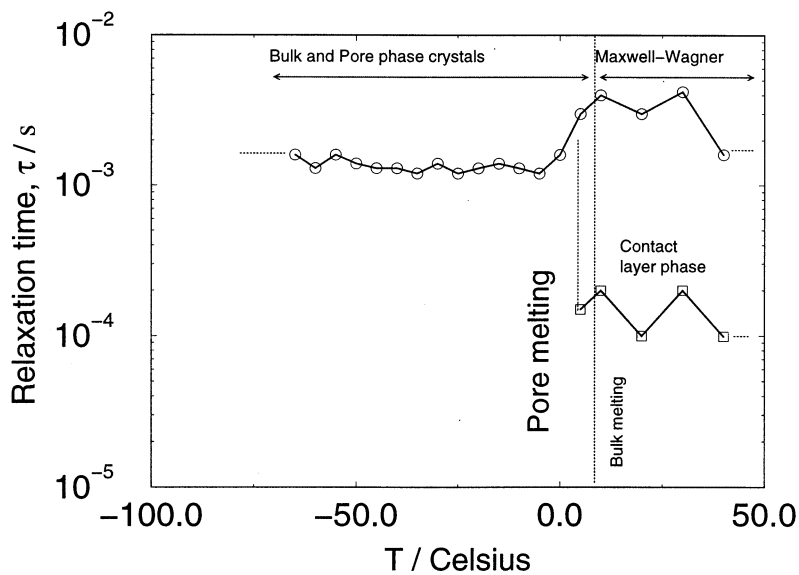

Fig. 2. Relaxation time vs. temperature for bulk nitrobenzene. At each temperature τ is estimated by fitting the dispersion spectrum to the Debye dispersion equation.

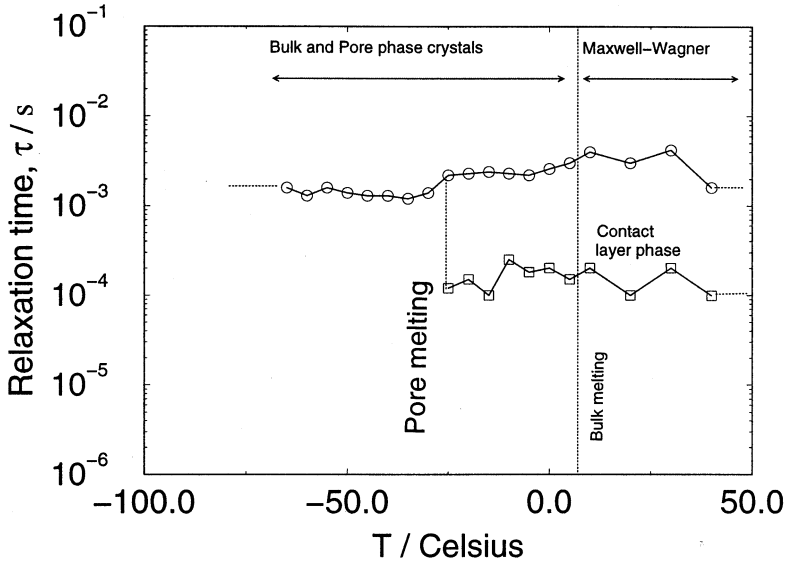

Fig. 3. The behavior of κ_r vs. T for nitrobenzene in a CPG material with an average pore diameter of 25 nm. The sample is introduced as a suspension of porous glass particles in bulk nitrobenzene. Thus, the signals are for both bulk and confined nitrobenzene.

behavior in κ_r vs. ω, and a double maximum in κ_i vs. ω. The longer component of the relaxation that is of the order of 5×10^{-3} s is because of Maxwell–Wagner–Sillars (MWS) polarization. For a heterogeneous system there occurs a relaxation mechanism due to interfacial polarization, when a slightly conducting liquid is enclosed in an insulating material. This effect, called the MWS polarization [10], is known to have a relaxation time of the order of 10^{-3} s [11,12]. The shorter relaxation component, of the order of 50×10^{-6} s, is too slow to represent the liquid phase relaxation in the pore. However, it is known that for dipolar liquids confined in nano-scale pores, the molecules in the contact layer show a slower dynamics, with a relaxation time of the order of 10^{-5} s [11–13]. The shorter relaxation component is consistent with such a behavior of the contact layer. Thus, the 50×10^{-6} s branch of the relaxation time that occurs for temperature above 2°C (Fig. 2), corresponds to the response of the contact layer that is believed to be in an orientationally ordered (hexatic) state [14,15]. The response of the liquid phase in the bulk and the inner layers of the pore are not accessible in our experiments as sub-nanosecond relaxation times are not affected by the frequency range we use in our experiments. The disappearance of the 50×10^{-6} s branch of the relaxation time and the appearance of the 10^{-3} s branch at 2°C, points to the freezing of the liquid in the pores. Below this temperature, the millisecond relaxation time corresponds to the crystal phase relaxation in the bulk and in the pore. The MWS effect disappears because the CPG particles are arrested in the crystalline matrix of bulk nitrobenzene, thereby preventing interfacial dispersion. Thus, from Figs. 1 and 2, the melting temperature of the fluid inside the pore is determined to be 2°C.

3.3. Effect of pore-size

Fig. 3 shows the relaxation time τ, for the freezing of nitrobenzene in a 8.5 nm CPG material. The trends are qualitatively similar to that observed for the 25 nm pore. From the relaxation time behavior in Fig. 3, we estimate the melting temperature inside the pores to be -23°C (the temperature below which the microsecond relaxation disappears). The 10^{-3} s branch of the relax-

ation time in Fig. 3 is divided into three regions. The response in the region, $T > 6$°C is due to MWS polarization; $-23 < T < 6$°C corresponds to the relaxation of the bulk crystal and $T < -23$°C is due to the combined relaxation of the bulk crystal and the crystal inside the pores.

For average pore diameter $H \geq 8.5$ nm, the behavior of the relaxation time with temperature suggests that the crystalline phase in the pore is a homogeneous phase, i.e. molecules have a single relaxation component throughout the confined crystalline phase. For smaller pores however, e.g. Vycor with $H = 4.5$ nm, the behavior is quite different. Fig. 4 is a plot of the corresponding relaxation times for nitrobenzene melting in Vycor glass. The microsecond branch of the relaxation time shows a sharp increase at $T = -40$°C, which can be taken to be the melting temperature inside the pores. The millisecond branch is again divided into three regions, $T > 5.6$°C (MWS polarization), $-40 < T < 5.6$°C (bulk crystal phase) and $T < -40$°C corresponding to the crystalline phase relaxations in the bulk and in the pore. However, there is a new branch of relaxation times of the order of a few hundred nanoseconds which occurs below the melting temperature of nitrobenzene in the pores ($T < -40$°C). This strongly suggests that the confined crystalline phase in not homogeneous, but that there are regions that are glass-like (amorphous), having a relaxation component of the order of a few hundred nanoseconds. Thus for pore diameters as small as 4.5 nm, the confinement poses a serious constraint on the formation of a homogeneous crystalline phase in the pore. The exact structure of the confined crystalline phase cannot be determined from dielectric relaxation spectroscopy experiments alone. One would need to resort to more direct methods, such as X-ray diffraction or molecular simulation, in order to obtain the fluid structure of the inhomogeneous crystalline phase.

In Fig. 5 the melting behavior of nitrobenzene in a MCM-41 porous material having an average pore diameter of 2.8 nm is shown. The qualitative behavior is different from the behavior in Vycor. The freezing transition at low temperature is absent as the microsecond branch of the relaxation time does not show any discontinuity. Once again there is a branch of relaxation times of the order of a few hundred nanoseconds, suggesting the presence of amorphous regions. We conclude that the pore size of 2.8 nm is too small to accommo-

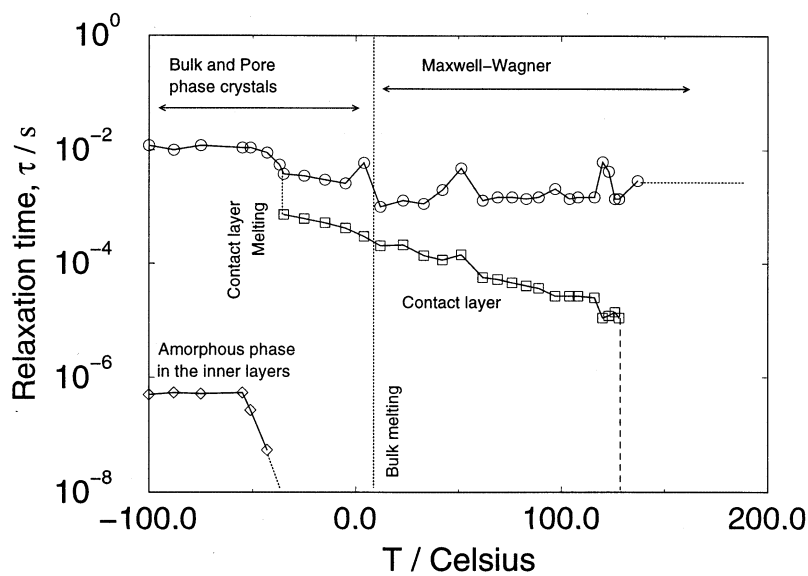

Fig. 4. Spectrum plot for nitrobenzene in a 25 nm pore at 20°C. The symbols correspond to experimental measurements and the solid and dashed curves are fits to the real and imaginary parts of Equation 2, respectively.

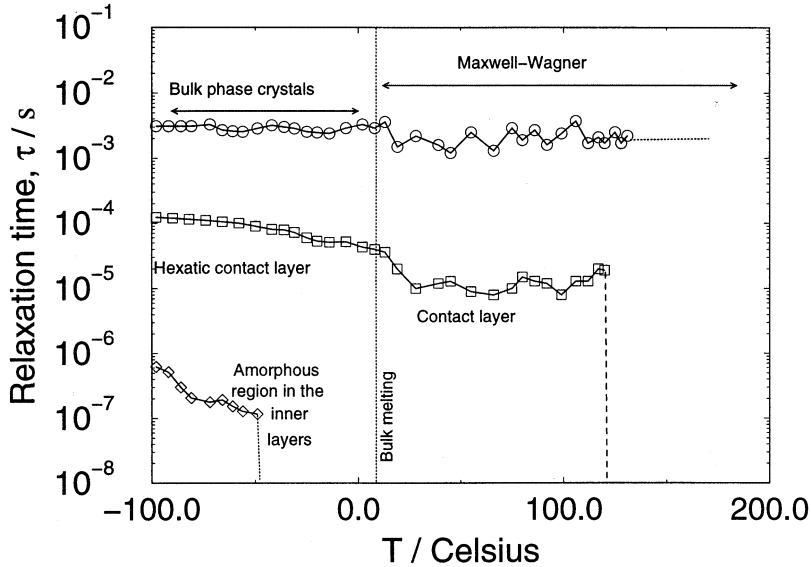

Fig. 5. Spectrum plot for nitrobenzene in a 25 nm pore at −10°C. The symbols correspond to experimental measurements and the solid and dashed curves are fits to the real and imaginary parts of Equation 2, respectively.

date even a partially crystalline phase. The contact layer remains in an orientationally ordered phase, while the inner region undergoes a glass transition. A very similar behavior is observed for the case of nitrobenzene inside an MCM-41 material of pore diameter 2.4 nm. Table 1 summarizes the melting behavior of nitrobenzene for a range of pore sizes in various silica-based pores. Nitrobenzene freezes to a crystalline structure when confined in pore sizes $H \geq 8.5$ nm ($H \geq 17\sigma_{ff}$). For a pore size of 4.5 nm, only part of the fluid freezes, with the rest forming an amorphous phase. For pore sizes smaller than 2.8 nm, the confined fluid does not undergo a freezing transition, however a glass transition is observed.

4. Discussion and conclusions

Recently, the freezing behavior in slit-shaped pores has been understood in considerable detail [4]. In the case of freezing in cylindrical geometry, the qualitative behavior has some similarities to freezing in slit-shaped pores. However, there are two important differences. First, the freezing temperatures in a cylindrical pore are in general lower than a slit pore of the same porous material and pore size [3]; this is because the adsorbate is confined in two dimensions rather than one, make it more difficult for the molecules to arrange themselves on a lattice. Second, in the case of slit-shaped pores, a freezing transition is observed (resulting in a homogeneous crystalline confined phase) for all pore sizes down to the smallest pore size, which accommodates only one molecular layer of adsorbed molecules [16,17]. In the case of cylinders, however, our experiments show that a homogeneous crystalline confined phase results

Table 1
Freezing temperatures: experimental measurement

H (nm)	H (σ_{ff})	T (°C)	Ordered phase
Bulk	∞	5.8	Crystal
25 (CPG)	50	2.0	Crystal
8.5 (CPG)	17	−25	Crystal
4.5 (Vycor)	9	−40	Crystal + glass
2.8 (MCM-41)	5.6	−50	Glass
2.8 (MCM-41, Al)[a]	5.6	−65	Glass
2.4 (MCM-41)	4.8	−65	Glass

[a] Five percent of Si atoms replaced by Al, by doping the sample.

only for cylindrical pores with average diameters larger than 20 σ_{ff}. For cylindrical pores with diameters in the range $12 < H/\sigma_{ff} < 20$, the confined phase at low temperature is an inhomogeneous phase with partially crystalline domains interspersed with amorphous regions. For cylindrical pores with $H \leq 12\ \sigma_{ff}$, the confined phase at low temperature consists of an orientationally ordered (hexatic) contact layer and an amorphous inner region.

Recently, Sliwinska-Bartkowiak et al. [14] reported a molecular simulation study that involved the calculation of the free energy surface using Landau theory and bond-orientational order parameter formulation. For spherical Lennard–Jones molecules in smooth cylindrical pores, they found that the confined phase crystallized into a frustrated fcc crystal structure (with defects) for pore diameters greater than 20 σ_{ff}. The thermodynamic freezing temperature was also located by calculating the grand free energy of the liquid and crystalline phases as a function of temperature. The authors also found that for a pore diameter of 15 σ_{ff}, the low temperature phase consisted of a contact layer that was crystalline (the in-plane, quasi-two-dimensional pair correlation function in the contact layer corresponded to a hexagonal crystal) with the inner region being amorphous throughout [14]. For pore diameters smaller than 12 σ_{ff}, the authors found the low temperature phase to be amorphous throughout [14]. These findings are consistent with our experimental results.

There are obvious differences in surface roughness and chemical heterogeniety between CPG, Vycor and MCM-41 samples. However the results from the molecular simulation study of Sliwinska-Bartkowiak et. al. [14] suggest that the differences in freezing behavior for CPG, Vycor and MCM-41 observed in our experiments are primarily due to the difference in pore size.

Acknowledgements

It is our pleasure to thank Kuni Morishige for helpful discussions. This work was supported by grants from the National Science Foundation (Grant No. CTS-9908535) and KBN (Grant No. 2 PO3B 175 08), and by a grant from the US–Poland Maria Sklodowska-Curie Joint fund (grant no. MEN/DOE-97-314). Supercomputer time was provided under a NSF/NRAC grant (MCA93S011).

References

[1] L.D. Gelb, K.E. Gubbins, R. Radhakrishnan, M. Sliwinska-Bartkowiak, Rep. Prog. Phys. 62 (1999) 1573.
[2] M. Miyahara, K.E. Gubbins, J. Chem. Phys. 106 (1997) 2865.
[3] M. Maddox, K.E. Gubbins, J. Chem. Phys. 107 (1997) 9659.
[4] R. Radhakrishnan, K.E. Gubbins, M. Sliwinska-Bartkowiak, J. Chem. Phys. 112 (2000) 11048.
[5] W. Haller, J. Chem. Phys. 42 (1965) 686.
[6] T. Elmer, in: S. Schnider (Ed.), ASM Engineered Materials Handbook, ASM, Materials Park, OH, 1991, p. 427.
[7] I. Nowak, M. Ziolek, in: M. Rozwadowski (Ed.), Third Polish–German Conference, Nicholas Copernicus University Press, Torun, 1998, p. 161.
[8] M. Sliwinska-Bartkowiak, R. Sikorski, J. Gras, R. Radhakrishnan, L.D. Gelb, K.E. Gubbins, Langmuir 15 (1999) 6060.
[9] A. Chelkowski, Dielectric Physics, Elsevier, New York, 1980.
[10] G. Bánhegyi, J. Coll. Int. Sci. 264 (1986) 1030.
[11] P. Pissis, A. Kyritsis, D. Daoukakri, G. Barut, R. Pelster, G. Nimtz, J. Phys. Condens. Matter 10 (1998) 6025.
[12] J. Schüller, R. Richert, E. Fischer, Phys. Rev. B 52 (1995) 15232.
[13] M. Urbakh, J. Klafter, J. Phys. Chem. 97 (1993) 3344.
[14] R. Radhakrishnan, K.E. Gubbins, M. Sliwinska-Bartkowiak, R. Sikorski, G. Dudziak, R. Gras, 2000 (in press).
[15] R. Radhakrishnan, K.E. Gubbins, M. Sliwinska-Bartkowiak, Phys Rev Lett 2000 (submitted).
[16] R. Radhakrishnan, K.E. Gubbins, Mol. Phys. 96 (1999) 1249.
[17] R. Radhakrishnan, K.E. Gubbins, A. Watanabe, K. Kaneko, J. Chem. Phys. 111 (1999) 9058.